A Flexibility Management System for Providing Close-to-real-time Power Services: An Experimental Case Study in PVZEN Microgrid Lab

Smart Grids and Sustainable Energy (2026) 11:13
https://doi.org/10.1007/s40866-026-00325-0

CASE STUDY

A Flexibility Management System for Providing Close-to-real-time Power Services: An Experimental Case Study in PVZEN Microgrid Lab

Jose-Fernando Forero-Quintero[1] · Alessandro Ciocia[2] · Roberto Vilafafila-Robles[1] · Filippo Spertino[2] · Francisco Díaz-González[3,4]

Received: 7 November 2025 / Accepted: 8 January 2026

Abstract

This paper presents a novel flexibility management system to handle short-term power deviations generated by intrinsic variability in generation and demand, and behind-the-meter flexibility provision in a close-to-real-time framework (30-second intervals). The proposed system employs an adaptive autoregression algorithm as a short-term forecast of energy exchange to the grid and a cost-benefit analysis to adjust the power setpoints of the energy devices by means of redispatching and unit reassignment modules. Experimental case studies are conducted in the PVZEN microgrid laboratory to validate the proposed system, testing critical scenarios and diverse flexibility requests. The results confirm the optimal management of the power deviations and the techno-economic feasibility of flexibility supply with real-world equipment, reducing the total operation cost from 11% to 85% compared to the baseline scenario. Finally, findings of previous studies based on simulations are verified experimentally, validating the influence of variables such as sample frequency, aging cost models, and flexibility price.

Keywords Close-to-real-time · Flexibility · Smart grid · Experimental case

Introduction

The growing penetration of renewable energy sources into the electricity generation mix requires increasing levels of flexibility in the power system [1, 2]. Such flexibility is defined as the ability to adapt to ongoing volatility in generation and demand in a technically and economically viable way [3]. Considering the meter and the Point of Interconnection (POI), flexibility is addressed from two perspectives, front-of-meter [4], and behind-the-meter [5]. In the first one, external agents such as Distribution System Operator (DSO) or balance responsible party, seek to directly modulate the power output of the energy assets to supply flexibility services [6]. For instance, studies have evaluated the flexibility of front-of-meter photovoltaic plants [7] or battery energy storage systems [8] connected to T&D network to provide diverse ancillary services to the grid. Conversely, the behind-the-meter flexibility is managed by end-users, or by an aggregator on their behalf [9], to optimize the user's electricity consumption. This optimization is centered on a specific energy asset or all available Distributed Energy Resources (DERs). The most common DERs are Electric Vehicle (EV), stationary batteries, Photovoltaic Panels (PV),

Alessandro Ciocia, Roberto Vilafafila-Robles, Filippo Spertino contributed equally to this work.

✉ Jose-Fernando Forero-Quintero
jose.fernando.forero@upc.edu

Alessandro Ciocia
alessandro.ciocia@polito.it

Roberto Vilafafila-Robles
roberto.villafafila@upc.edu

Filippo Spertino
filippo.spertino@polito.it

Francisco Díaz-González
francisco.diaz-gonzalez@upc.edu

[1] Centre d'Innovació Tecnològica en Convertidors Estàtics i Accionaments, Electric Engineering Department, Universitat Politècnica de Catalunya-BarcelonaTech, Av. Diagonal 647, Pav G, Barcelona 08028, Spain

[2] Dipartimento Energia "Galileo Ferraris", Politecnico di Torino, Corso Duca degli Abruzzi 24, Torino 10129, Italy

[3] Department d'Enginyeria Elèctrica, Universitat Politècnica de Catalunya, Av. Diagonal 647, Barcelona 08028, Spain

[4] Serra Húnter Fellow, Barcelona, Spain

Published online: 20 February 2026

controllable loads (water heaters, air conditioning systems, and other programmable or deferrable appliances), among others. The aggregator is a recent actor in the power system, which aims to accumulate enough flexible capacities from end-users to participate in energy markets on behalf of its stakeholders.

For behind-the-meter flexibility, energy management and control can be raised from two approaches: power management [10–13], and flexibility management [14–16]. In general, these approaches differ in their objective functions. First, energy resource optimization revolves around reducing electricity costs and generating revenue through lower electricity prices or by utilizing excess renewable energy. Second, the provision of flexibility services seeks specific incomes based on its own capabilities to reduce or increase consumption and the needs of electricity sector stakeholders. Here, flexibility is usually characterized by the behavior of a flexible electrical parameter. Positive and negative flexibility are defined as the increase or reduction of an electric variable during a time period [17].

The provision of the behind-the-meter flexibility involves diverse steps, starting with its proper quantification and characterization. In prosumer cases, for example, a methodology based on the load shedding is proposed in [18] to calculate the flexibility potential. In the literature, multiple methods are available for various energy sectors, assets, and normative environments. Later, this flexibility potential must then be transformed into flexibility offers that can be traded on local [19] and [20] national energy markets as flexibility (ancillary) services. A procedure to solve this offering cost-efficient problem is shown in [21] for households with PV on their roof. Approved offers arrive at the energy management and control system to be executed in real-time.

In the context of electric microgrids, the control architecture must be adapted to handle flexibility requests, from external agents and internal actors appropriately. According to [22] and [23], two control levels must be executed during a microgrid's steady-state grid-connected operation mode. First, a high-level control is the Energy Management System (EMS), which produces an optimal power scheduling of the microgrid energy assets for long-term horizons, distributing power setpoints each medium time slot, hourly, half-hourly, or quarter-hourly [13]. Secondly, a low-level control also generates power setpoints for the assets, in terms of seconds or minutes, within the EMS's time slots. Here, the main objective is to control real-time power deviations to avoid critical situations, such as energy injection into the grid or exceeding the maximum threshold power, and minimize the electricity bill.

In the literature, several authors have presented diverse low-level control systems for microgrids to manage close-to-real-time power and energy. However, their time horizon, frequency sample, forecasting period, or calculating time is under 10 minutes, 15 minutes, or even one hour. In addition, most of these management systems are tested on a simulation platform, where relevant considerations, such as the required time to receive, process, and communicate information to the assets, aging costs of storage devices, and real-time deviations in generation and demand, among others, are often overlooked. Therefore, this work deepens the proposal realized in [24], about a novel close-to-real-time (30-second-interval-based) energy management system named Flexibility Management System (FLEMS), complementing and unifying its control and optimization architecture, as well as testing its effectiveness in an experimental case study. In this work, savings from 11% to 85% are yielded in the energy bill, and providing flexibility to the network successfully.

The remainder of the paper is organized as follows: Section 2 shows a short review on close-to-real-time energy management system. Section 3 delves into the control structure and mathematical formulation of the proposed FLEMS. A description of the PVZEN microgrid laboratory is performed in Section 4. Three case studies on power control and flexibility supply, along with their results are presented in Sections 5 and 6, respectively. Finally, conclusions and future work are exposed in Section 7.

Review on Close-to-real-time Energy Management System

According to the literature, there are two approaches to manage and control energy in microgrids: power management and flexibility provision. Regarding management approaches, research articles focused on power management aim to generate an optimal energy dispatch plan, composed of power setpoints for DERs (e.g., stationary batteries), based on generation and weather forecasts, consumption patterns, and energy prices, among others factors. [10] and [25] generate an optimal power dispatch through hourly setpoints for the next 24 hours. [13] and [26] go further and propose an EMS with setpoints every 15 minutes and incorporate environmental parameters and the aging model of storage equipment, achieving savings from 30% to 50 % of the end-user's electricity bill. Meanwhile, [11] proposes a management system that acts quickly (seconds) to correct short perturbations, returning to the initial power scheduling.

On the other hand, works focusing on the flexibility provision seek to determine new power setpoints for DERs that enable the fulfillment of power or energy requirements, according to the load and generation forecasts, real-time

power dispatch, aggregator instructions, and trade power techniques, among others. [14] delves into load forecast models to improve the accuracy of power setpoints, aiming to increase feasibility and hence, more flexibility. [12] studies the maximization of the ramping capacity of the microgrid, in 10-minute periods, to provide it as flexibility to the aggregator. At the same time, [5] proposes a peer-to-peer market-based control strategy to trade power between prosumers and supply flexibility at the point of connection in a coordinated manner.

Works in [12, 15], and [16] attempt to tackle the two management approaches together, in a two-stage or hierarchical system. The minimum required response time is 10 minutes at best, but it could be achieved in 30 minutes or even hours. All the above-mentioned works employ a simulation platform to validate and obtain their results. Conversely, [16, 27], and [28] use real equipment but without considering any flexibility request, as they focus on the stability of hybrid microgrids and optimization of the plug-and-play system for EVs, respectively. Table 1 summarizes the review of energy management systems for microgrids with DERs mentioned in this section.

It is important to highlight that there are multiple testbeds and laboratory platforms to carry out simulations, emulations or experiments with real equipments for microgrids, according to the literature. Four levels are defined by [29] according to use of aggregation software globally (Level 1), or by emulation groups (i.e, generation, storage and loads) (Level 2), each DER and its components (Level 3), or specific electric variable (Level 4). On the other hand, three different microgrid configurations are identified in the previous works, which depends on the type of central bus, direct current (serie), alternate current (parallel) or both using a switching mechanism (switch) [30].

At the same vein, each DERs has diverse mathematical models to simulate its behavior, emulation levels to mimic the performance of a real resource and real setups, which can be classified at the same levels as for microgrid emulation. For the sake of summarize, Table 2 show a review of the microgrid emulation testbeds and its configurations in the literature, including the emulation levels of the DERs implemented in each reference.

In conclusion, the PVZEN microgrid laboratory enables the execution of experiments with real-world equipment, ensuring proper performance, quality, and reliability among the set of microgrid testbeds, leveraging tangible generation, conversion, control, and communication energy assets.

According to the above-presented literature review, the main contributions of the present work is to handle both power management and flexibility provision in a unified way (as seen in Table 1) for a close-to-real-time framework (seconds), employs real-world equipment in a qualified microgrid laboratory to validate the feasibility of its technical and economic implementation (as shown in Table 2) , and the particular emphasis given to the Cost-Benefit Analysis (CBA), which plays a central role in assessing the practical relevance and advantages of the proposed approach.

Flexibility Management System

The goal of the proposed flexibility management system is to find the cost-optimal solution that reduce the extra costs incurred for real-time power deviations while complying with the flexibility provision. To do that, this work raises an unified management approach, which consists of two information and process flows, as illustrated in Fig. 1. The proposal is linked to the IEEE Standards, which define the specifications of microgrid controllers, classifying them into high- and low-level controllers, EMS and FLEMS, respectively.

Table 1 Review on close-to-real-time energy management system

	Timeframe			Approach			Case Study		
Ref.	[s]	[min]	[hr]	Power Manage- ment	Flexibility provision	Unified	Simula- tion	Emula- tion	Real-world equipment
[5]		X		X	X		X		
[10]			X	X			X		
[11]	X			X			X		
[12]		X		X	X		X		
[14]		X			X		X		
[13]		X		X			X		
[15]			X	X	X		X		
[27]	X			X					X
[16]			X	X	X				X
[28]	X			X					X
[25]			X	X			X		
[26]		X		X			X		
[24]	X			X	X			X	
[Present work]	X					X			X

Table 2 Review on microgrid emulation testbeds

			DER				Microgrid config		
Ref.	Case Study	Emulation Level	Battery	PV	EV	Load	Series	Paralel	Switch
[5]	Simulation	1	3	3	–	1		X	
[10]	Simulation	3	1	1	4	1	X		
[11]	Simulation	3	1	3	–	3		X	
[12]	Simulation	1	1	1	–	1		X	
[14]	Simulation	1	1	1	–	1		X	
[13]	Simulation	3	3	3	3	3		X	
[15]	Simulation	3	3	–	3	3		X	
[27]	Real	3	Real	Real	Real	3			X
[16]	Real	1	1	1		1		X	
[28]	Real	3	Real		Real	Real		X	
[25]	Simulation	1	1	1	–	1		X	
[26]	Simulation	3	3	3	–	3		X	
[24]	Emulation	3	3	3	3	3		X	
[Present work]	Real	3	Real	Real	3	Real		X	

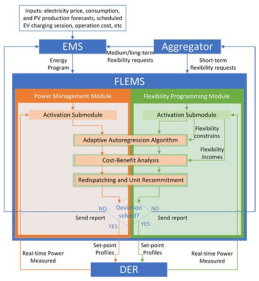

Fig. 1 Flexibility management system flowchart

On the one hand, the Power Management Module (PMM) encompasses an optimal procedure to calculate and preserve the optimal power program (orange). This module is carried out by FLEMS taking into account the optimal energy programm, generated by EMS, for the assets on a rolling horizon (e.g., 1 day), composed of a series of power setpoints commonly divided into time intervals (T) of 15 minutes (96 values) or 30 minutes (48 values). The EMS considers multiple parameters, such as the historical and forecast energy generation of the DERs, electricity consumption and price, State of Charge (SoC), battery's power, and energy requirements of the EV charging sessions [13]. Such optimal scheduling is transmitted both to the FLEMS to establish some reference values in the activation submodule and DERs via inverter.

On the other hand, the Flexibility Programming Module (FPM) entails a strategy to handle long, medium, and short flexibility requests, which involves the aggregator, EMS, and FLEMS (green). The accepted offers are sent from aggregator to the EMS to update its optimal energy program. Unlike PMM, FPM aims to provide behind-the-meter flexibility by controlling extra costs and power deviations that occur in real-time. FPM can move away from the EMS power optimum schedule towards a local optimum, but seeks to return to EMS's schedule since it represents the overall power optimum. Thus, the control and management system combines energy optimization for the end-user and cost-effective flexibility provision.

The unified management approach starts with a pair of activation submodules, which have the same structure but with modifications in the corresponding algorithms to add some technical and economic aspects to the flexibility disposal, which will be discussed in the following sections. Later, three submodules are stringed, Adative Autoregression Algorithm (ARA), CBA, and redispatching and unit recomitment submodules, to predict the real-time state of assets, evaluate the cost-optimal solution and ajust the solution to the particular restrictions. These submodules will be addressed in the next sections. The final power setpoints are communicated to the DERs to be executed in real-time. Finally, when the deviations are very large and exceed the FLEMS capacity, a report is sent to the EMS and aggregator so that the corrective actions can be taken.

Activation Submodules

The activation submodules are responsible for defining the reference power values of the DERs based on the optimal points received from EMS. They also calculate the power absorbed from the grid at the POI and the expected consumption, as well as the initial values of the associated cost for Operation and Maintenance (O&M) for battery (Com_t^{bat}) and EV (Com_t^{ev}), aging cost for battery (Cag_t^{bat}) and EV (Cag_t^{ev}), and PV curtailment cost Cur_t^{pv}. The term t represents the FLEMS's sample time. Later, the calculation of the costs are based on real-time power measurements. If a flexibility requirement is received $Pflx_t$, an auxiliary binary variable $Rflx_t$ is

activated to indicate the flexibility provision to the subsequent submodules. This study focuses on the technical and experimental reliability of the behind-the-meter flexibility provision. Therefore, requirements managed by FLEMS will always be assumed to be previously agreed upon and accepted offers.

In addition, the activation submodules also apply the Traffic Line Concept (TLC) [31], which prioritizes instructions (power management, flexibility supply, or other operation modes) depending on the real-time power balance. When the grid is operating normally (green light), the energy market operation takes priority, preferring the economic savings of prosumers. System operators, aggregators, or prosumers can temporarily require flexibility to avoid unstable grid status or provide an ancillary service (yellow light). Whereby the flexible behavior of consumers must seek reliability over the economic benefit of optimizing consumption or existing generation. In unstable permanent grid states (red light), system operator can override contracts, take control of energy assets, and execute emergency actions. For this study, the activation submodules move between green and yellow states in response to the receipt of a flexibility request.

Finally, the zero-injection constraint is challenging not only in terms of flexibility but also for any DER-based energy management system. Currently, there are three main solutions for zero-injection in on-grid inverters. The first solution involves a sub-metering scheme applied in the control and communication systems to measure energy consumption in real-time [32]. The meter detects any energy injection and notifies the inverter, which must adjust the output power of its DGs accordingly. This solution relies on robust and efficient communication systems. The second approach typically involves using minimum or reserve power, particularly in commercial applications [33], where it prefers to buy energy from the grid rather than risk a penalty for exceeding the minimum power. Defining an appropriate power amortization rate is essential. This rate should consider factors such as consumption variability, penalties, maximum power limits, the flexibility of energy assets, and electricity prices. Lastly, a control system based on per-phase control is utilized, especially in three-phase systems, to monitor the average power among the three phases [34]. When one phase's power is lower than the others, that phase becomes the reference point, and the inverter manages the remaining phases to align with this baseline value.

For this work, the issue of zero-injection is addressed through a power reserve ratio [32]. The power rate is included in this submodule and is equal to 5% of the maximum power, in other words, 95 W, which is a proper value for residential prosumers according to [35].

Adaptive Autoregression Algorithm Submodule

The Adaptive Autoregression Algorithm (ARA), the central axis of this submodule, is used as a short-term forecasting method to predict the electricity consumption to the grid at the POI. ARA averages the deviations of the past values concerning the optimal reference values from EMS, generating a correction factor for the next optimal value in the next time slot.

The Algorithm 1 summarizes the steps and functioning of the ARA submodule. The inputs are the real-time measured power at time *t-n* (P^{RT}_{t-n}), forecasted power at time *t* done at time *s* by EMS ($P^{EMS}_{t,s}$), forecasted power at time *t-n* done at time *t-s* by EMS ($P^{EMS}_{t-n,s-n}$), and weight coefficients φ_n. The coefficients φ_n model the impact of past deviations on the forecast. These coefficients are part of intelligent forecasting methods, which have proven to be more efficient and accurate than statistical or persistence methods [36]. Currently, support vector machines (SVN) and artificial neural networks (ANN) are the most widely used machine learning algorithms for calculating these types of coefficients related to consumption behavior. For example, SVNs are used to predict the coefficients of the autoregressive part of a easonal autoregressive integrated moving average (SARIMA) model to predict energy consumption based on 1- to 2-year datasets [37]. In general, such coefficients are found utilizing historical data about consumption behavior, error series, and indexes of accuracy, among others factors. In fact, the training process is not the subject of this study and can be further explored in future work.

On the other hand, ARA determines a penalty if the power forecasted by FLEMS surpasses the allowed maximum or minimum powers. These penalties are transmitted to the CBA submodule to include them in the cost-benefit analysis.

Algorithm 1 Adaptive autoregression ARA.

Require: $P^{,EMS}_{t,s}$, P^{RT}_{t-n}, φ_n, $P^{,EMS}_{t-n,s-n}$
Ensure: $P^{,FLEMS}_{t,t-1}$
1: Record historical data to feed a train procedure
2: **Calculate** φ_n **for** $n = 1, ..., min(N, s)$
3: $P^{,FLEMS}_{t,t-1} \leftarrow$ **from Eq 1, for** $t = 1, ..., T$
4: **if** $P^{,FLEMS}_{t,t-1} < P_{min}$ **then**
5: **apply** $Penalty_{min}$
6: **else**
7: **if** $P^{,FLEMS}_{t,t-1} > P_{max}$ **then**
8: **apply** $Penalty_{max}$
9: **else**
10: **end if**
11: **end if**
12: **return** $P^{,FLEMS}_{t,t-1}$, $Penalty_{min}$, $Penalty_{max}$

The mathematical formulation of ARA algorithm, based on [38, 39], is expressed in Eq. 1, where $P^{FLEMS}_{t,t-1}$

corresponds to the forecasted power at time t done at time t-1, s is the EMS time execution, N is the number of previous time intervals.

$$P_{t,t-1}^{FLEMS} = P_{t,s}^{EMS} \frac{1}{min(N,s)} \left(\sum_{n=1}^{min(N,s)} \varphi_n \frac{P_{t-n}^{RT}}{P_{t-n,t-s}^{EMS}} \right) \quad (1)$$

Cost-benefit Analysis Submodule

After forecasting power at POIs using the ARA, FLEMS employs a Cost-Benefit Analysis (CBA) to find adjustment powers for each DER that minimize the extra costs associated with deviations between forecast and actual values [24]. CBA estimates all costs and revenues associated with real-time power dispatch and flexibility provision and compares them with the forecast values found by EMS and FLEMS in the ARA submodule.

The Algorithm 2 summarizes the CBA stages. The extra cost is estimated by multiplying the Italian market tariff scheme for residential households, X_t, with the total power deviation, which is calculated as the difference between the powers predicted by FLEMS, $P_{t,t-1}^{,FLEMS}$, and EMS, $P_{t,s}^{,EMS}$. Here, $P_{t,t-1}^{,FLEMS}, Penalty_{min}, Penalty_{max}, X_t$ are found in Algorithm 1.

Algorithm 2 Cost benefit analysis CBA.

Require: $P_{t,t-1}^{,FLEMS}, Penalty_{min}, Penalty_{max}, X_t$ ← **from Algorithm 1, for** $t = 1, ..., T$
Ensure: **MINIMIZE** min f(t) costs function
1: $Cur_t^{pv}, Com_t^{bat}, Cag_t^{bat}, Com_t^{ev}, Cag_t^{ev}$ ← **Eq. 4-9 for** $t = 1, ..., T$
2: **Calculate:** $C_t^{FLEMS}, Ct_t^{bat}, Ct_t^{ev}$ **for** $t = 1, ..., T$
3: **Solve eq 2** ← Nonlinear programming solver.
4: **return** $Pbat_t^{FLEMS}, Pev_t^{FLEMS}, Ppoi_t^{FLEMS}$

Costs and revenues are calculated with the Eq. 2-5.

$$min \sum_{t=1}^{T} ((P_{t,t-1}^{,FLEMS} - P_{t,s}^{,EMS} + Pflx_t \; Rflx_t) * X_t + C_t^{FLEMS} - Iflx_t * Rflx_t) \quad (2)$$

With,

$$C_t^{FLEMS} = Ct_t^{bat} + Ct_t^{ev} + Cur_t^{pv} \quad (3)$$

$$Ct_t^{bat} = Com_t^{bat} + Cag_t^{bat} \quad (4)$$

$$Ct_t^{ev} = Com_t^{ev} + Cag_t^{ev} \quad (5)$$

Here, this work incorporates the flexibility variables, power ($Pflx_t$), binary variable ($Rflx_t$), and flexibility incomes ($Iflx_t$) into the equations in [24] to analyze the profitability of flexibility provision. X_t is the Italian market tariff scheme for residential households. The behind-the-meter flexibility costs are established as the difference between the total flexibility expenses, C_t^{FLEMS}, and the incomes, $Iflx_t$. The flexibility price is determined by DSO or aggregator through contractual agreements or energy markets. The price of the flexibility offer, per kWh, must be adequately reckoned in future works for capacity, availability, and energy delivered. The obtained results are the adjustment powers for the energy assets $Pbat_t^{FLEMS}$, Pev_t^{FLEMS}, $Ppoi_t^{FLEMS}$, which must be added or subtracted from the power set-points issued by the EMS.

The Eq. 2 describes the objective function of a Mixed-Integer Nonlinear Programming (MINLP) problem, which is used to optimize the adjustment power of each DER. For instance, FLEMS could determine, from an economic dispatch standpoint, whether a power deviation due to reduced photovoltaic production is offset by increased grid consumption, increased battery discharge, or a reduction in the duration of the EV charging session. The Eq. 3 - 5 outline the O&M cost for battery (Com_t^{bat}) and EV (Com_t^{ev}), aging cost for battery (Cag_t^{bat}) and EV (Cag_t^{ev}), and PV curtailment cost Cur_t^{pv}.

Regards to C_t^{FLEMS}, a quadratic cost models is implemented to calculate O&M cost of the storage devices such as battery and EV. The Eq. 6 describe the mathematical formulation for this model.

$$Com_{t,q} = a_c * (P_t)^2 + c \quad (6)$$

Where, P_t is the real-time active power of ESS for discharging and charging, a_c and c are quadratic and independent parameters defined by [40]. Eq. 7-9 outline the formulation for the aging cost model applied in this work, which corresponds with the Aging Cost Model 1 (ACM1). ACM1 is selected due to the higher savings it offers compared to other models. This model is based on the aging effect of a particular cycle in relation to the nominal cycle recommended by manufacturer (Ah_t^{ESS}), where Q, X, C_{life}, $IK_{t,SOCt}$ and I_{nom} are rated capacity in Ah, market price, life cycle, measured current at given $SOCt$, and nominal current of energy storage device, respectively.

$$Cag_{t,1} = X * \frac{Ah_t}{Q * C_{life}} \quad (7)$$

$$Ah_t = \frac{1}{T} * \int_0^T \sigma(IK_{t,SOCt}) * Ik_t \, dt \quad (8)$$

$$\sigma(Ik_{t,SOCt}) = \frac{\int_0^T Ik_t \, dt}{\int_0^T I_{nom} \, dt} \quad (9)$$

Redispatching and Unit Recommitment Submodule

The Redispatching and Unit Recommitment Module (RUM) is designed to address critical conditions that may require adjusting the DER's power set-point profiles to resolve issues such as voltage violations, reactive power dispatching, planned and unplanned islanding, reconnection, black start, and short-term flexibility requests. Given these scenarios, the ARA and CBA optimization modules need to be updated in real-time dispatching to reflect the new conditions. This study will focus specifically on the management of short-term flexibility requests concerning the maximum and minimum power exchanges at POI.

The RUM utilizes the same objective function described in the Section 3.3. This function aims to minimize energy costs and cost overruns during real-time dispatching, taking into account that the power set-point profiles of some DERs are fixed and predetermined within the CBA. Additionally, constraints are updated to ensure flexibility provision in spite of these changes. The updated CBA is solved using a restricted non-linear multivariate function library from Matlab® (*fmincon* function) [41].

PVZEN Microgrid Laboratory

Description of the Laboratory Equipment

The PVZEN laboratory [42] is equipped with three PV generators; their combined nominal power is 11.1 kWp, utilizing mono-crystalline silicon modules rated at 370 Wp and with 21.4% efficiency. The arrays are installed under non-optimal conditions, with azimuth angles deviating from the ideal southern orientation, and a fixed tilt angle of approximately 10°, representative of typical rooftop installations. Specifically, the PV generators include: one array of 12 modules (rated power, P_{peak}=4.44 kW) oriented at $-64°$ (SE), one array of 6 modules (P_{peak}=2.22 kW) at 116° (North-West), and a third array of 12 modules (P_{peak}=4.44 kW) split into two sub-arrays with the same respective orientations. Figure 2 shows the PVZEN real-world equipment.

A scheme of the main components of the PVZEN laboratory, including the three units and their connection to the grid, is represented in Fig. 3.

Each one of the three prosumers is equipped with lithium-ion batteries, with a nominal energy capacity, C_B=9.6

Fig. 2 Real-world equipment of the PVZEN microgrid laboratory. Batteries and inverters (right side), and PV panels (left side)

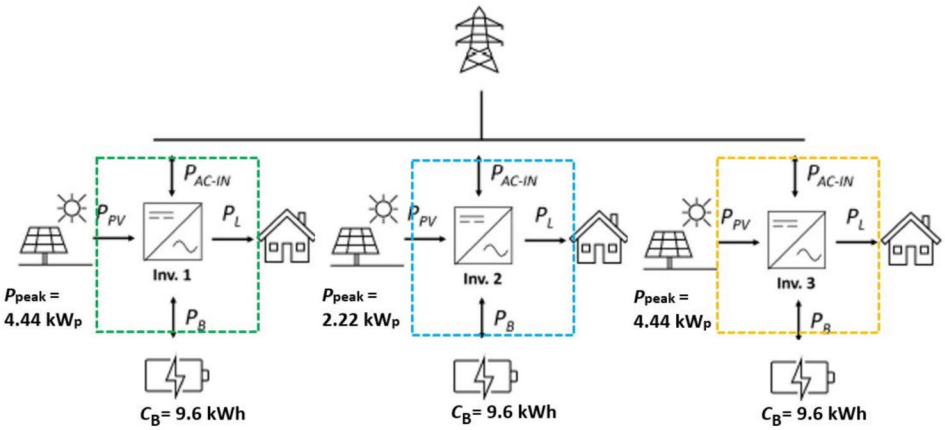

Fig. 3 Single-line diagram of the PVZEN microgrid laboratory.

kWh per prosumer [43]. The batteries operate at 48 V with a charge capacity of 50 Ah, supporting a maximum one-minute current of 100 A, and a Depth of Discharge (DoD) of 90%. Power conversion is handled by a 5 kW bidirectional converter per each prosumer, capable of both grid-connected and off-grid operation.

In Fig. 4,the internal architecture of the off-grid inverter is illustrated, highlighting the bidirectional conversion stage that interfaces the battery bank, the photovoltaic inputs and the AC terminals. The diagram shows the variables in each inverter. P_{AC-IN}, P_L, P_{PV}, P_B represents the power from the grid, loads, PV and battery, respectively. The embedded Energy Manager supervises the operating mode of the inverter, coordinating the power flows among PV generation, battery charging and load supply. The system also includes a monitoring unit capable of providing instantaneous power measurements and historical energy data, enabling real-time supervision of the overall microgrid operation [44]. The AC interface operates at 230 Vrms, 50 Hz.

In addition to the photovoltaic, storage and conversion units, the PVZEN microgrid includes a programmable electrical load emulator used to reproduce the consumption patterns of residential end-users. The load emulator is composed of resistive elements with forced-air cooling and can be remotely controlled via Modbus. Each load channel can dissipate up to 4 kW, allowing the laboratory to reproduce realistic demand profiles such as those of heat pumps or time-varying household appliances. The power absorption of each channel is continuously monitored and logged together with the rest of the DER measurements, ensuring consistency with the EMS and FLEMS control loops. To provide a consolidated overview of all the relevant devices in the experimental setup, Table 3 summarizes the key electrical parameters of the microgrid's main components, including the photovoltaic panels, battery units, off-grid inverters and programmable loads.

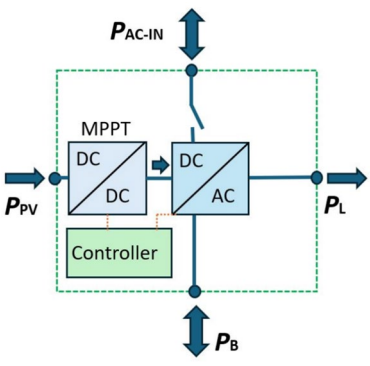

Fig. 4 Internal schematic of the inverter

Table 3 Electrical specifications of the PV modules, charge controller, storage units, inverters and programmable loads in the PVZEN microgrid

Component	Parameter	Value
PV modules — STC parameters		
	Maximum power $P_{\max}$	370 W
	MPP voltage V_{mpp}	37.0 V
	MPP current I_{mpp}	10.01 A
	Open-circuit voltage V_{oc}	42.8 V
	Short-circuit current I_{sc}	10.82 A
	Efficiency η_{mod}	21.4%
	Power tolerance	$0 \sim +3\%$
PV modules — Operating conditions		
	Temperature range	$-40^{\circ}\mathrm{C} \sim +90^{\circ}\mathrm{C}$
	Max system voltage	1000 V
	Max series fuse rating	20 A
PV modules — Temperature coefficients		
	NOCT	$44 \pm 3^{\circ}\mathrm{C}$
	Power coefficient	$-0.30\%/^{\circ}\mathrm{C}$
	Voltage coefficient	$-0.24\%/^{\circ}\mathrm{C}$
	Current coefficient	$+0.037\%/^{\circ}\mathrm{C}$
PV charge controller (MPPT)		
	Battery voltage	48 V
	Number of MPPT inputs	4
	Max module current (per channel)	13 A
	Open-circuit module voltage	180 V
	Max input power per channel	900 W
	Total PV input power	4.6 kW
	Efficiency	97.2%
	Self-consumption	12 mA
Battery storage units		
	Nominal capacity	9.6 kWh (8.64 usable)
	Nominal voltage	48 V
	Max discharge current	100 A
	Round-trip efficiency	94–96%
	BMS update interval	0.5–1.0 s
Off-grid inverter		
	Nominal output power P_{out}	5000 VA
	Max output power	10000 VA
	Battery voltage	48 V
	Output voltage	230 V
	Output frequency	50 Hz
	Overload threshold	85%
	Efficiency η	95%
Load emulator		
	Number of units	3
	Max power per unit	$\approx$4 kW
	Cooling	Forced-air
	Control interface	Modbus
	Logging interval	1 s

Description of the Data Acquisition, Processing, and Control System

The PVZEN laboratory is equipped with a multilayer data acquisition, processing, and control infrastructure designed to provide reliable monitoring and to enable real-time interaction with both the EMS and the FLEMS (Fig. 5). All devices communicate using the MODBUS TCP/IP protocol over a dedicated local Ethernet network, while lower-level field connections rely on MODBUS RTU over RS-485 links. A supervisory software module continuously polls the inverters, battery systems, and load emulators, retrieves their registers, organizes the raw measurements, and stores them in a structured SQL database hosted on a server located inside the laboratory. The communication parameters have been configured to ensure stable acquisition timing; MODBUS RTU operates at 9600 bps, a baud rate widely used in industrial settings because it offers a robust trade-off between noise immunity and throughput, especially over shielded RS-485 cabling. Since the distance between laboratory components is limited to several tens of meters, this configuration ensures almost error-free communication without requiring repeaters or line-conditioning devices [45]. MODBUS TCP/IP polling is executed with a 1-second refresh cycle, matching the sampling rate of the power analyzers and enabling unified time stamping across all data streams.

In addition to internal measurements, an external acquisition module periodically retrieves environmental data such as irradiance measurements, weather forecasts, and historical datasets from sources such as PVGIS [46]. All internal and external data streams are merged into a unified dataset used by the analytics and control software. This software layer performs data filtering, aggregation, synchronization, and preprocessing, generating the inputs required for both the EMS forecasting routines and the real-time optimization executed by FLEMS. A core feature of the system is its closed-loop control capability. After processing the available measurements, the control module computes set-points for inverters, battery units, and load emulators, and transmits them back to the physical devices via MODBUS TCP/IP. Experimental characterization of the sensing–decision–actuation loop confirms that the end-to-end response time is well below the 30-second control interval adopted by FLEMS. Further details on the timing performance and related measurements are provided in Section 6. This ensures that the physical microgrid remains fully synchronized. To support real-time supervision and the computation of key performance indicators, all relevant measurements are also streamed to a Grafana-based monitoring environment [47]. This provides continuous visualization of the microgrid's operating conditions, including power flows, SoC evolution, environmental variables, and system-level KPIs.

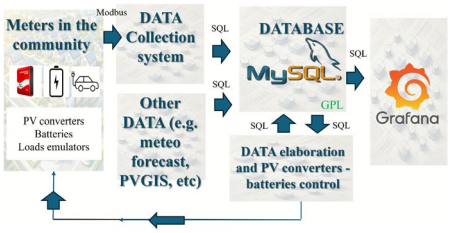

Fig. 5 Architecture of data collection and microgrid management in the PVZEN laboratory

Case Studies

Description

Using the energy assets installed in the PVZEN microgrid laboratory, three experimental case studies have been designed to test the proper functioning of the management system proposed in this work. The first two case studies analyze the operation of a single prosumer under critical conditions for power management (Case Study 1) and flexibility provision (Case Study 2). The third case study evaluates the coordinated behavior of the three prosumers, as an energy community, for flexibility supply (Case Study 3).

The inverter power optimizer serves as a reference for comparing the decisions made by FLEMS, as the inverter solves the power flow in real-time, thereby assuming the last received power set points. This optimizer, by default, seeks to reduce the energy consumption of the grid as much as possible, even injecting electricity into the grid. For all case studies, three events could occur due to variability of electricity consumption and generation, which are as follows:

- PV Curtailment: FLEMS establishes a limit of 500 Wh as tolerable solar curtailment due to forecast deviations in PV production. When this limit is exceeded, FLEMS reformulates the power set-point for PV panels.
- Unexpected EV Charging session: An unexpected EV charging session is scheduled at various times. FLEMS optimizes the associated cost overrun, avoiding surpassing the redefined maximum power at POI (1900 W).
- Undesired active power exchange with the network: Possible energy injections into the grid could take place during the analyzed period, according to the variation of the inflexible consumption and real-time PV production.

Finally, FLEMS's parameters have been selected as a reference case, for which PVZEN's microgrid will be executed

for all case studies. This reference scenario facilitates comparison of results across different case studies. These parameters are summarized in Table 4.

Methodology

Figure 6 summarizes the experiment execution process used to configure the case studies. Initially, EMS is executed at time *t-s*. EMS produces optimal power setpoints for DERs in quarter-hourly intervals for the next day, considering the approved medium/long-term flexibility request from an external agent (e.g., an aggregator) and its optimization variables (electricity price, pollutant emissions, etc.). Such power setpoints are sent to PVZEN's inverters and the FLEMS through the data collection system shown in Fig. 5. Inverters update their energy program for each DER.

A period before real-time execution (*t-1*), inverters solve the current power flow according to EMS setpoints, manufacturer criteria, and real-time measurement. Meanwhile, FLEMS reads the real-time values, receives the agreed-upon short-term flexibility request, and produces the adjustment powers to minimize extra costs and guarantee the flexibility provision. Later, FLEMS and inverters unify the power setpoints, which are registered in the inverters for real-time power dispatch (*t*). Ultimately, if the real-time situation exceeds FLEMS' adjustment capacities, a report is generated for the aggregator or DSO to inform them about the situation and explore possible solutions.

Lastly, continuous monitoring of power quality, including voltage and frequency variations, as well as harmonic distortions in voltage and current, is performed during the execution period of each experimental test. The objective of this verification is to identify potential impacts on power quality resulting from actions taken by the energy management systems (EMS and FLEMS), which could limit the effectiveness of management decisions.

Table 4 FLEMS's reference parameters for PVZEN's microgrid

Definition	Value
Sample time	$t = 30$ s
EMS's time intervals	$T = 15$ minutes
Number of measured past values	$N = 3$
EMS's execution time	$s >> N$
Weight coefficients	$\varphi_n = 1$, for $n = 1, ., min(N, S)$
Cost function	Quadratic formula
Aging Cost Model	ACM1 [24]
ACM1's quadratic factor	a_c= 2 €/kW^2
ACM1's lineal factor	c= 1 €
Maximum power at POI	P_{max}= 1900 W
Power amortization rate for zero injection	$Pzero = 5$ %
Power reserve for zero injection	$Pres = 95$ W
Penalty for exceeding the max power	$Pen_{max} = 1.4064$ €/kWh
Penalty for surpassing the min power	$Pen_{min} = 2$ €/kWh
Penalty for energy not supplied (EV)	$Pen_{ev} = 5$ €/kWh

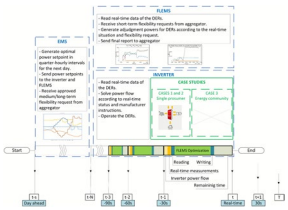

Fig. 6 A schematic of the experiment execution process

Single Prosumer

Case Study 1

From the PVZEN microgrid laboratory, Inverter 1 (Unit 1) is used as a single-family prosumer. The EV charging sessions are programmed using the virtual building available in the PVZEN lab, which utilizes information collected from DataPort Inc. Street 2022 for residential prosumers [48]. For this case study, the hypothetical contracted power is 1.9 kW, impeding any sell-back electricity to the grid. For CBA, the Italian dynamic electricity tariff is applied, neglecting its power term value and taxes. EMS was executed at 16:00 the day before the FLEMS execution, conserving the condition $s >> N$, where **s** corresponds with time before real-time when EMS was executed, and **N** is the collected time before real-time according to the number of past values used by FLEMS.

Case Study 2

Like Case Study 1, Unit 1 is configured as a low-voltage AC residential prosumer. To test the flexibility capabilities of FLEMS, positive and negative flexibility offers have been prepared in accordance with the EMS's forecasts and flexibility potential. Before the delivery time of flexibility, such offers must be previously identified, informed, traded, and approved by EMS, aggregator, or external agent. Consequently, these stages are often overlooked, as it is assumed they are successfully completed when FLEMS receives manageable offers. FLEMS's reference parameters are applied in this case, aggregating an award rate for flexibility supplied equal to 2 €/kWh for positive and negative offers, according to [49]. The maximum and minimum DoD come flexible if there is an active flexibility request.

Energy Community

Case Study 3

Here, the three single inverters are combined to reproduce three single grid-connected prosumers as three single-family energy community. This case study aims to prove the effectiveness of FLEMS in managing flexibility requirements. Each inverter receives a request to either reduce or augment its consumption to the grid, based on the real-time conditions of the inverters. The profits for flexibility provision were estimated at 2 €/kW as a reference price, according to [49]. Again, scheduled and unexpected EV charging sessions are lined up through virtual buildings. The ARA parameters and cost models details correspond with the values defined for Case Study 1 for each inverter.

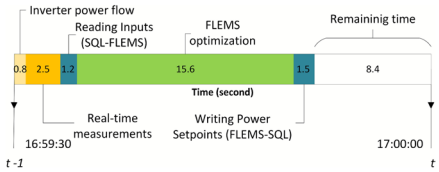

Fig. 7 Net time required for managing power of PVZEN microgrid

Results

The results presented in this Section were obtained during an experimental activity conducted over a four-month period, during which several experiments were performed under different operating conditions and flexibility requests. Among the entire dataset, the time frames reported in Figures 7, 8, 9, 10, 11, 12, 13, 14, 15, 16, 17, 18, and 19 were selected as representative examples, since they capture the most critical situations and illustrate the effectiveness of the proposed approach. For the sake of simplicity, only these relevant intervals are presented and discussed in detail.

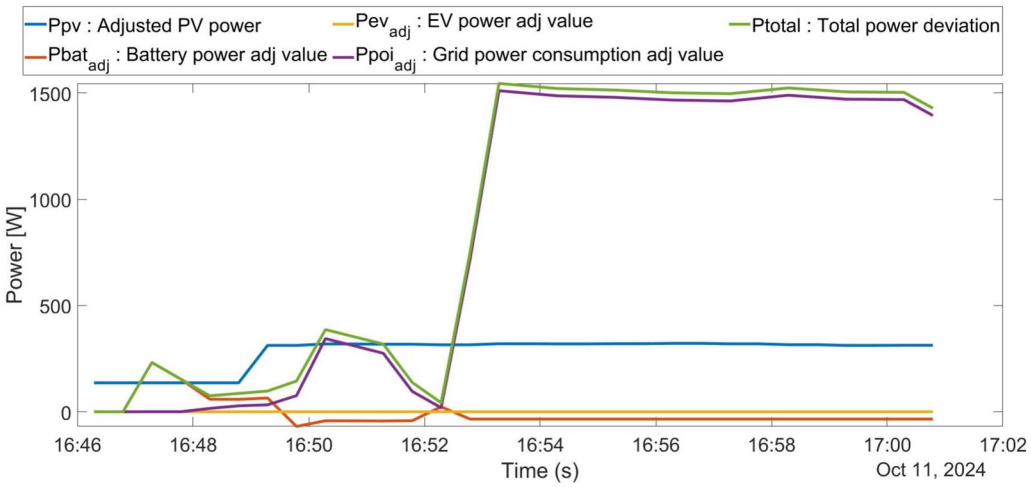

Fig. 8 Case study 1: FLEMS power adjustments for energy assets

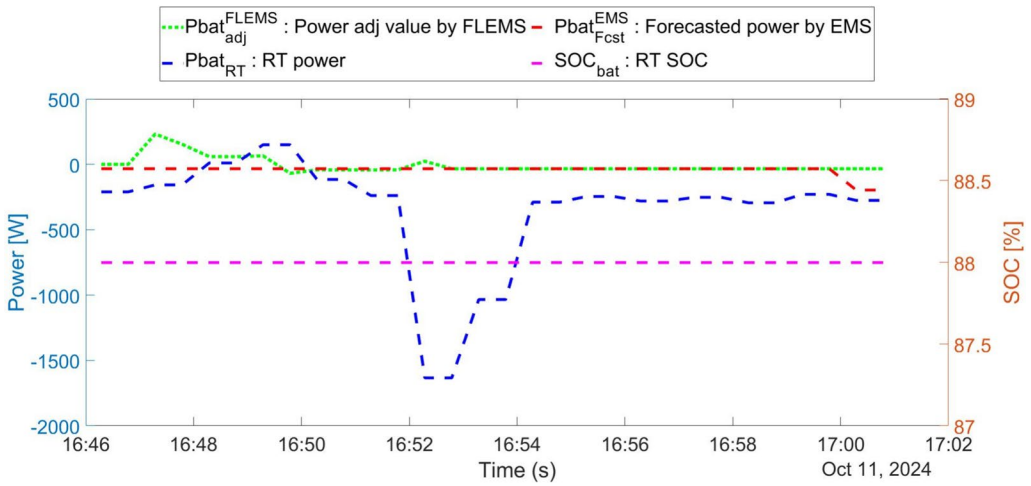

Fig. 9 Case study 1: Real-time battery power comparison

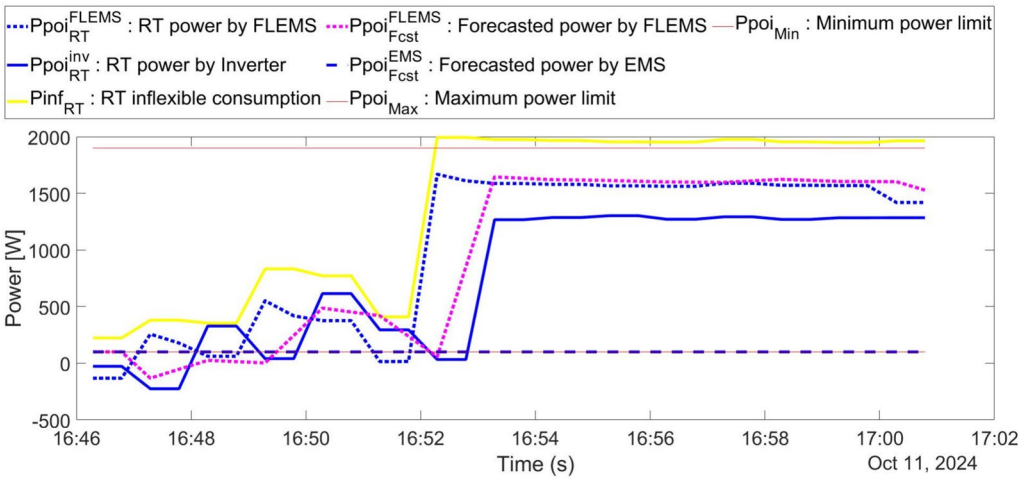

Fig. 10 Case study 1: Real-time power exchange comparison at POI

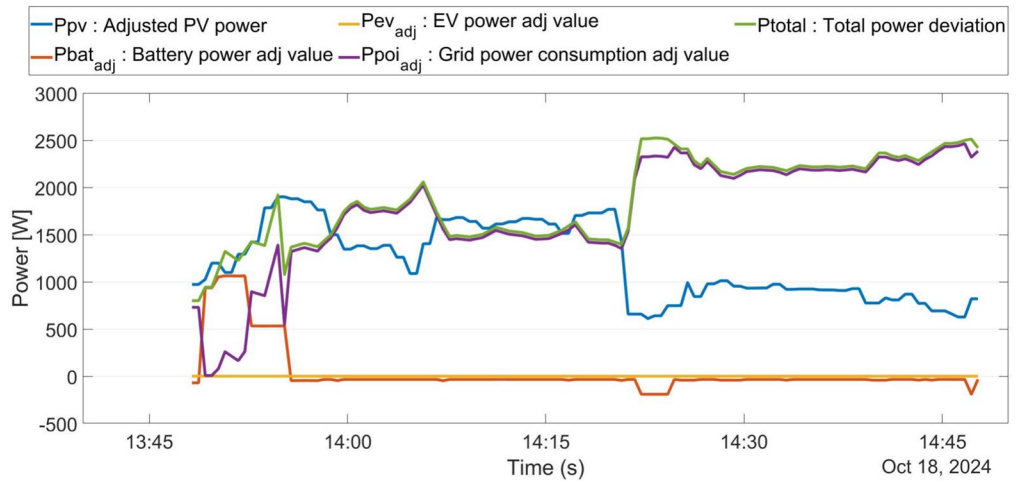

Fig. 11 Case study 2: FLEMS power adjustments for energy assets

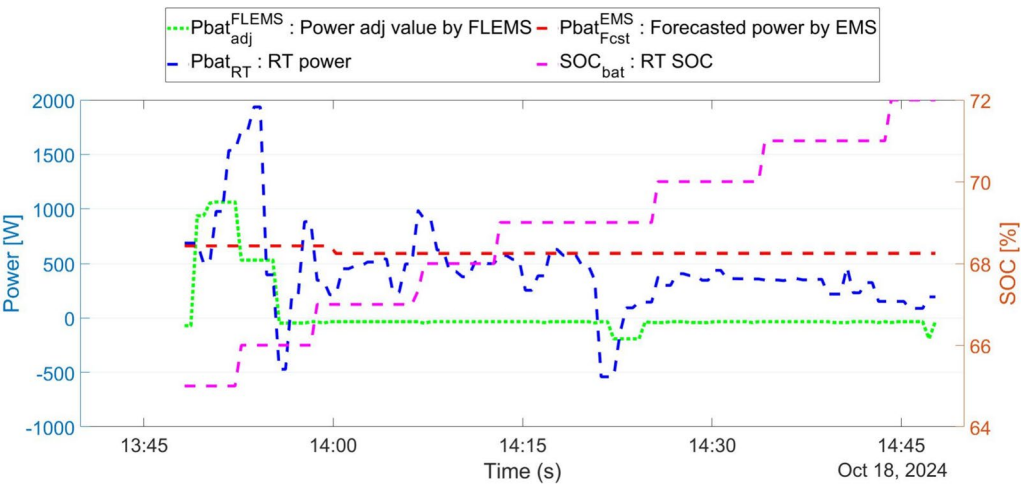

Fig. 12 Case study 2: Real-time battery power comparison.

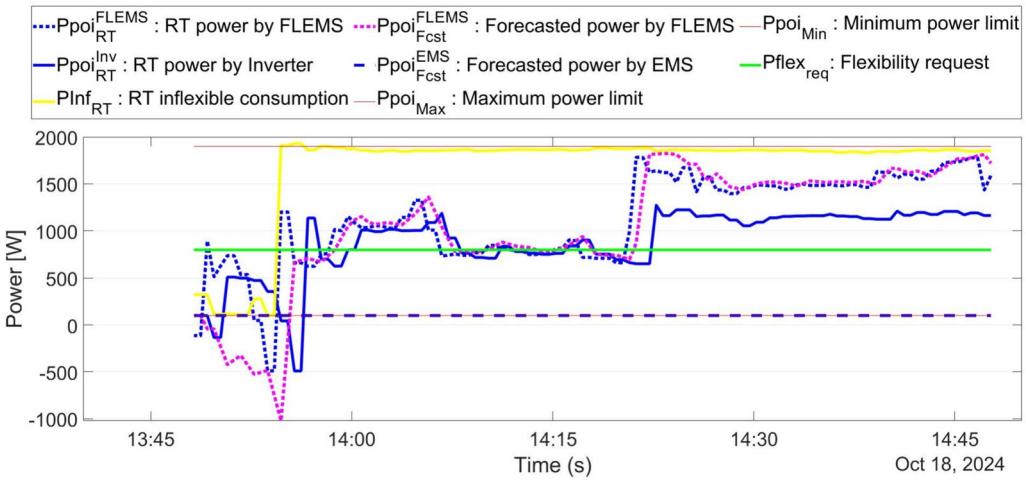

Fig. 13 Case study 2: Real-time power exchange comparison at POI under flexibility provision scenario

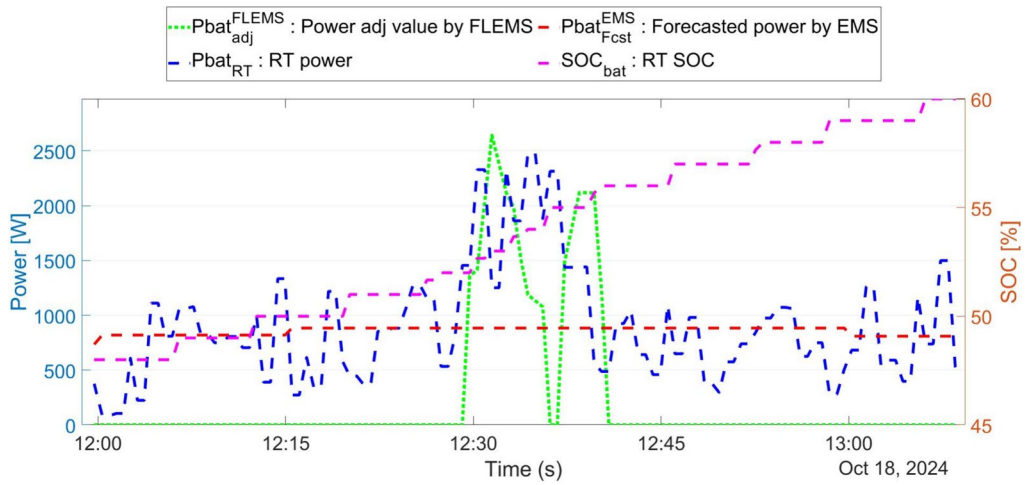

Fig. 14 Case study 3: Real-time battery power comparison in Unit 1

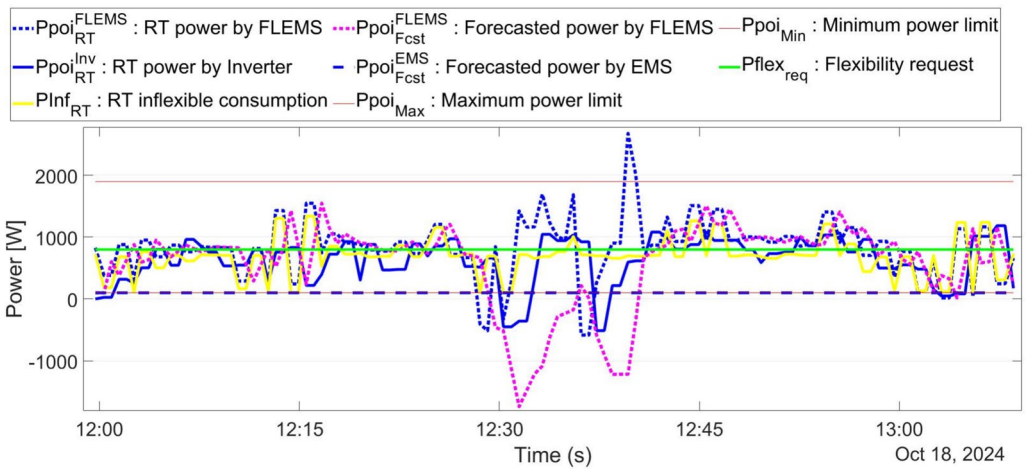

Fig. 15 Case study 3: Real-time power exchange comparison at POI under flexibility provision scenario in Unit 1

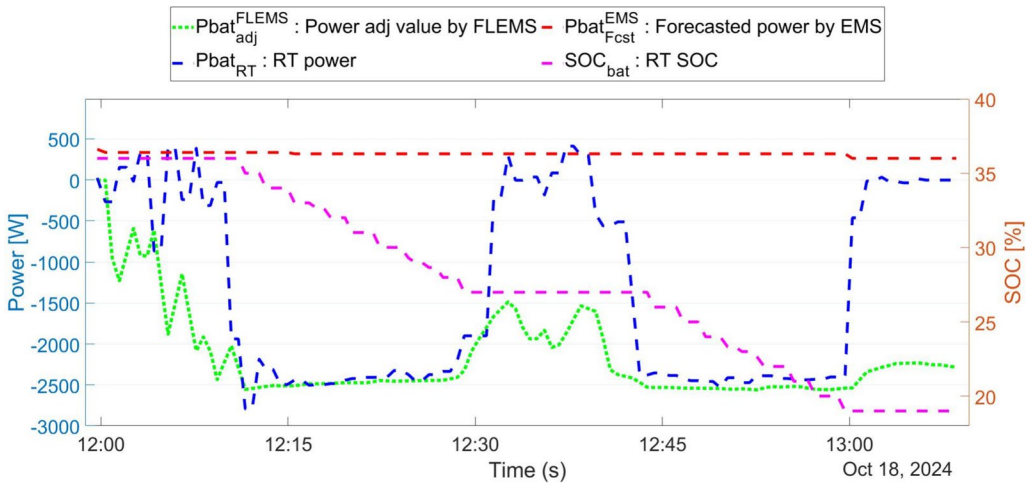

Fig. 16 Case study 3: Real-time battery power comparison in Unit 2

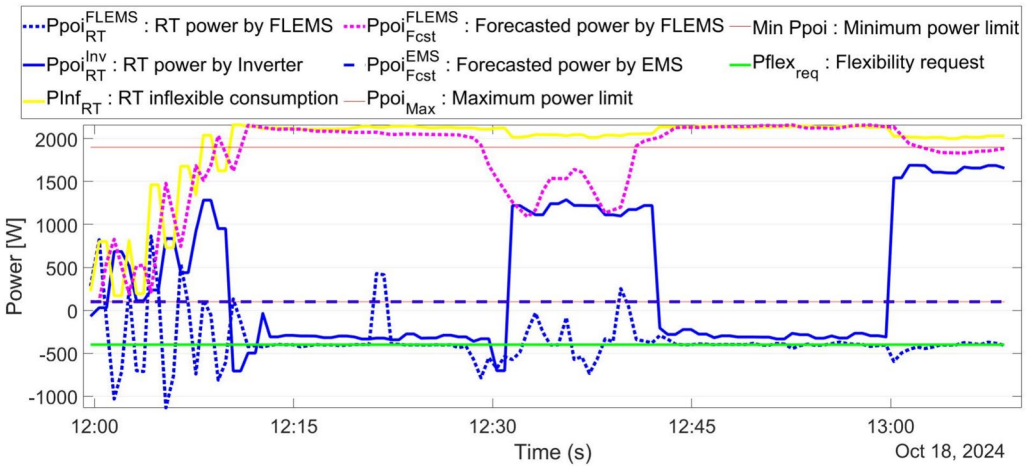

Fig. 17 Case study 3: Real-time power exchange comparison at POI under flexibility provision scenario in Unit 2

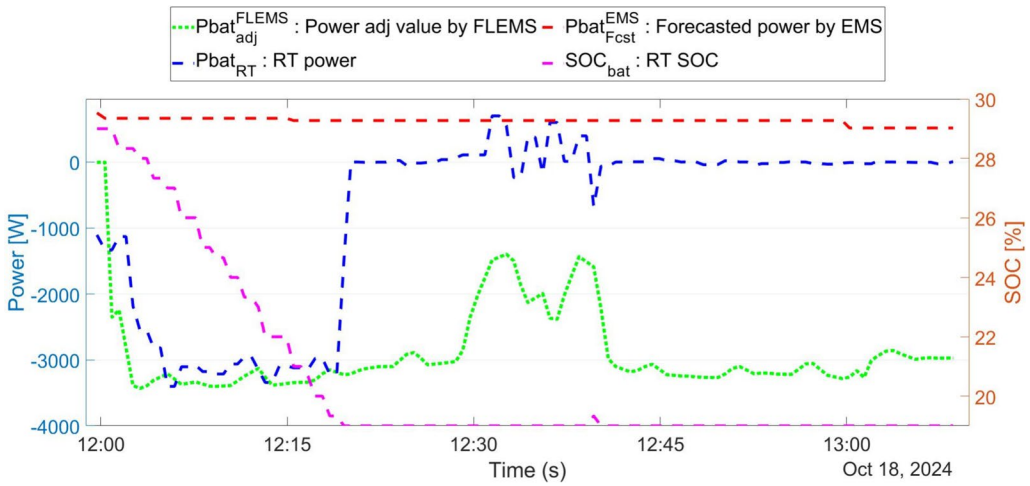

Fig. 18 Case study 3: Real-time battery power comparison in Unit 3

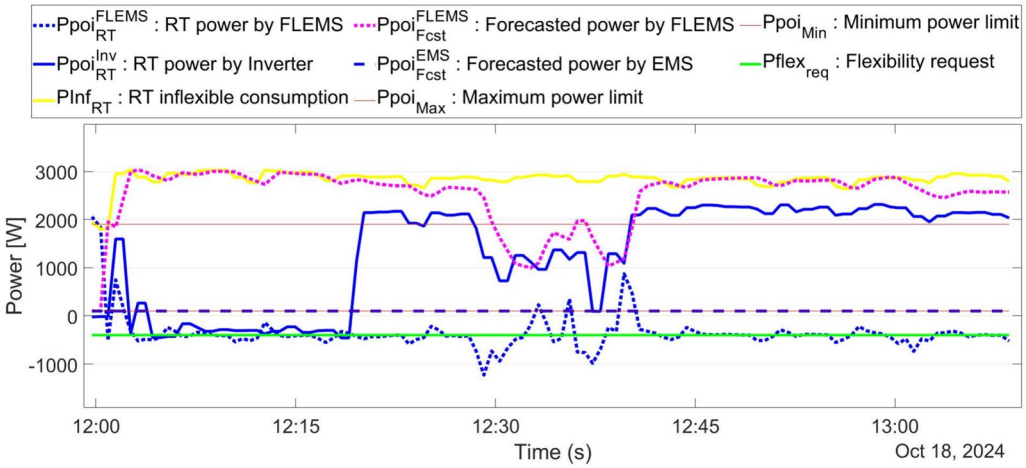

Fig. 19 Case study 3: Real-time power exchange comparison at POI under flexibility provision scenario in Unit 3

As a departure point, the FLEMS sampling rate was set at 30 s to avoid measurement overlaps caused by implicit latency for data reading and writing, communication, recording, and processing. These latencies directly depend data management, transmission and processing systems of the PVZEN microgrid laboratory. In this way, the experimentally observed time rates are summarized in Fig. 7, and defined as follows:

- Power flow solution by inverter: 0.8 s.
- Recording real-time measurements on database: 2.5 s.
- Transmission and reading of input data from SQL database to FLEMS: 1.2 s.
- Execution of the FLEMS's optimization: 15.6 s.
- Transmission and reading of input data from FLEMS to SQL database: 1.5 s.
- Remaining time before power flow solution: 8.4 s.

It is worth mentioning that the EMS operates daily at 16:00, after the electricity price is known, and the transmission of the set points for the following 24 hours takes, on average, approximately 42 minutes, using the same communication, transmission, and information management structure (SQL).

Single Prosumer

Case study 1 analyzes the FLEMS's behavior under the intrinsic volatility of consumption and DG, as well as unexpected events related to close-to-real-time power dispatch. Besides, it examines the FLEMS's response to an approved flexibility requirement within the same context of energy uncertainty. As a reminder, EMS previously generated an optimal energy program for each asset for all case studies. This schedule involves the previous forecasting process of electricity consumption and PV production, expected EV charging sessions, electricity prices, and validated flexibility offers.

Power Management (Case study 1)

Regarding the study of the optimal operation of a single prosumer, Fig. 8 shows the power adjustments for energy assets generated by FLEMS. Here, FLEMS adjusts the EMS's power setpoints according to the total deviation power (*Ptotal*) as defined in Section 3.3. Initially, there is a power deviation at the POI, caused mainly by an excess of PV energy in relation to the EMS's forecasting (about 140 W) and real-time production (about 320 W). To avoid energy injections to the grid, especially when the EMS forecasted power is equal to the minimum allowed power (Fig. 10, solid red line, $Ppoi_{Min}$), FLEMS charges the battery from 16:46:07 to 16:49:47 to a maximum of 231 W (Fig. 8, solid orange line, $Pbat_{adj}$), taking into account that battery's SOC is within the operational range, from 20% to 90% (Fig.9, dashed purple line, SOC_{bat}). At the same time, FLEMS accounts for the PV curtailment until 16:48:47 when it reaches 500 Wh, where FLEMS sets a new power setpoint at 312 W (Fig. 8, solid blue line, *Ppv*). From 16:49:47 to 16:52:17, FLEMS discharges the battery at 42 W according to the new PV power and inflexible consumption (Fig. 10, solid yellow line, $Pinf_{RT}$).

An unexpected EV charging session occurs at 16:49:47. However, it is only reflected on the inflexible consumption curve at 16:52:17 due to delays in power switching in the resistance bank and the required time to register the new power setpoint in the inverter. With the EV's connection, the inflexible consumption suppers the 1900 W (Fig. 10, solid red line, $Ppoi_{Max}$). Due to the application of a penalty for exceeding the maximum power (2€/kWh), the

current state of the battery's SoC (88%), and a previous discharge approximately the same power at present time frame, FLEMS decides discharging the battery at 34 W until 17:00:47 whenever the PV excess persists and the real-time power at POI (Fig. 10, dotted blue line, $Ppoi_{RT}^{FLEMS}$) remains below of the maximum allowed power.

Figure 9 displays the real-time power of the battery during the resolution time. A relevant point here is the inverter's behavior in front of real-time power variations, as a comparison between FLEMS and inverter helps evaluate the FLEMS' performance. Initially, the inverter discharges and charges the battery (dashed blue line, $Pbat_{RT}$) around its forecasted power by EMS (dashed red line, $Pbat_{Fcst}^{EMS}$). In the face of the EV charging session, the inverter discharges the battery, reducing the electricity demand to 246 W until the end of the analyzed time. As shown in Fig. 10, the inverter permits injections into the grid, surpassing the minimum power limit (solid blue line, $Ppoi_{RT}^{Inv}$), especially during the first six minutes. Conversely, FLEMS avoids any power injection in relation to the forecasted power at POI (dotted purple line, $Ppoi_{Fcst}^{FLEMS}$) and follows the EMS power setpoints to diminish the battery degradation.

The total cost raised by FLEMS and EMS's execution is lower (0.01 €) than the allocated cost forecasted by EMS (0.079 €) or real-time total cost without FLEMS (0.082 €). This is mainly due to curtailment of photovoltaic output, exceeding the facility power thresholds, rejection of the EV charging session, and changes in battery usage patterns.

Flexibility Provision (Case study 2)

Figures 11, 12, and 13 expose the results of case study 2 related to flexibility management in a prosumer. As in the previous section, Fig. 11 presents the adjustments to the EMS's power setpoints done by FLEMS during the set time (from 13:48:13 to 14:47:42 on October 18, 2024). The programmed flexibility request is a positive requirement of 800 W, i.e. an increase in consumption (Fig. 13, solid green line, $Pflex_{req}$). Initially, FLEMS increases the battery charging power (Fig. 11, solid orange line, $Pbat_{adj}$) predefined by EMS (Fig. 12, dashed red line, $Pbat_{Fcst}^{EMS}$), from 660 W to 1722 W until 13:55:43. Accelerating the charging session of the battery is possible due to an energy excess of the PV that achieves maximum levels of 1900 W at 13:55:13 in relation to the forecasted production by EMS (972 W), as well as because the battery's SOC is within the working range (Fig. 13, dashed purple line, $Ppoi_{Fcst}^{FLEMS}$). At the same time, FLEMS modifies the PV power setpoint (1026 W) at 13:49:13, as solar overproduction is higher than the PV curtailment rate. All of these adjustments aim at the accomplishment of the flexibility request, which is fulfilled with some difficulty at 13:52:13 due to an influx of PV energy and the inflexible consumption reduction (Fig. 13, dotted blue line, $Ppoi_{RT}^{FLEMS}$). Conversely, to surpass this critical period, the inverter injects energy into the grid (491 W) for 2 minutes, much longer than the FLEMS (Fig. 13, solid blue line, $Ppoi_{RT}^{Inv}$).

As planned, an unexpected EV charging session starts at 13:54:13 (Fig. 13, solid yellow line, $Pinf_{RT}$). This EV's connection is authorized by FLEMS, adjusting the battery charging point to the predicted value by EMS, setting it to 660 W to stabilize electricity consumption around the flexibility requirement value. Later, FLEMS conserves the battery power setpoint from EMS until the end of the set time due to stability in the energy balance between the persistent PV energy excess, unexpected EV charging sessions, inflexible consumption and flexibility requests, except for two instances. Such instances occur when FLEMS must shift the EMS battery power (192 W) at 14:22:13 and 14:47:12, avoiding to exceed the maximum power (1900 W). These energy imbalances are caused by a decrease in PV production below the production predicted by EMS. For the same situation, the inverter continuously varies the battery power, attempting to reduce overall energy costs but violating the flexibility guideline and wearing out the battery with half-cycles of charge and discharge, especially at 14:06:43 and 14:21:13. Besides, the inverter moves away from the optimal points defined by EMS, which could cause additional costs in other time periods where a certain level of battery's SOC is required because of high electricity prices.

At last, the total cost associated with the FLEMS's management is 0.06 €for the 15-minutes under analysis. The costs estimated by EMS previously and real-time incurred costs without FLEMS's intervention are 0.41 €and 0.42 €, respectively. The above represents a saving of 85.36%. Enabling EV connectivity, managing excess PV production, and providing efficient behind-the-meter flexibility are key contributors to these savings. For the sake for comparison, current studies show that consumers can save between 10% and 20% on their electricity costs by arbitrage with competitive pricing, or demand management [50] (i.e, 4.5% in datacenters). Savings of 65% are achieve with energy management with transactive energy trading mechanism without real-time response or even 130% if the retributions for ancillary services to the grid are proper designed [51] (Case 1 and 2, respectively). Therefore, FLEMS enable increase potential savings and benefits.

Energy Community (Case study 3)

An energy community, formed by three inverters from the PVZEN laboratory microgrid, manages positive and negative offers assigned according to their batteries' SOC and predicted powers by EMS. A positive offer of 800 W is

assigned to Unit 1 (Fig. 15, solid green line, $Pflex_{req}$). Units 2 and 3 receive a negative offer of -400 W (Figs. 17 and 19, solid green line, $Pflex_{req}$) during the time frame (from 11:59:41 to 13:08:33 of October 18th, 2024). As stated above, these offers are assigned, assuming they have been correctly estimated, planned, and traded. Additionally, EV charging sessions are neglected in this case study.

Initially, Fig. 14 shows the battery power comparison in real-time for Unit 1. FLEMS maintains the battery's power setpoints done by EMS (dashed red line, $Pbat_{Fcst}^{EMS}$) until 12:29:07 because the increase of power consumed from the grid is generated by a decrease in PV generation to the same extent, taking into account the inflexible consumption (Fig. 15, solid yellow line, $Pinf_{RT}$). The above-mentioned is confirmed by the real-time battery power behavior executed by the inverter (Fig. 14, dashed blue line, $Pbat_{RT}$). From 12:29:07 to 12:39:03, two high peaks of PV generation occur (2820 W and 2757 W) with a duration of 7 and 3 minutes, respectively. Therefore, the electricity from the grid is reduced drastically. In consequence, FLEMS charges the battery at a higher power rate to follow the flexibility setpoint, given that the current battery's SOC (dashed purple line, SOC_{bat}) is less than the maximum one (95%). Both the inverter and FLEMS can not refrain from injecting energy into the grid, but FLEMS quickly restores the flexibility mandate. Later, FLEMS maintains the power setpoint determined by EMS until the end of the timeframe. The average power consumed from the grid with FLEMS was 830 W, above the FLEMS requirement.

Units 2 and 3 also experience the same initial drop in PV generation. Here, FLEMS must deviate from the power setpoint predicted by EMS and discharge the battery until 2453 W and 3389 W, respectively (Figs. 16 and 18, solid green line, $Pbat_{adj}^{FLEMS}$).These battery discharges must be increased according to the increase in the inflexible load and EMS power setpoints, 335 W and 663 W, respectively (Figs. 16 and 18, dashed red line, $Pbat_{Fcst}^{EMS}$) . The inverter proceeds in the same way as FLEMS, discharging the battery (Figs. 16 and 18, dashed blue line, $Pbat_{RT}$) aggressively. As a result of FLEMS's decisions, the POI's powers of Units 3 and 2 range around -400 W from 11:59:41 to 12:12:07 approximately. Meanwhile, such powers are moving away from the flexibility requirement by inverter, since it does not discharge the battery at the necessary power rate (especially in Unit 2) as shown in Figs. 17 and 19. Due to continuing PV generation deviation and the subsequent aggressive battery discharging, Unit 3 achieves the minimum SOC determined by the inverter (above 20%), which implies stopping the battery discharge and ignoring the flexibility requirement. This also occurs in Unit 2 but at 12:59:38. Conversely, FLEMS allows batteries to continue discharging at a higher DoD according to their CBA, where the additional aging cost is taken into account. In the context of flexibility requests, FLEMS changes the maximum DoD from 20% to 5%, thereby avoiding complete discharge of the battery. The two photovoltaic overgeneration peaks are resolved by FLEMS by reducing the battery discharge power, keeping the energy consumed from the grid within the flexibility limit. Finally, the average powers consumed from the grid of Units 2 and 3 with FLEMS were -368 W and -355 W, respectively.

Regarding the total operational cost associated with the energy community and flexibility requests, Table 5 summarizes the costs recorded in cases where the EMS power guidelines had been followed, power deviations had been allowed without FLEMS action, and FLEMS had been involved. Experimentally, FLEMS is key to accomplish the flexibility requirements. As shown in Table 5, FLEMS reduces the overall cost by approximately 11.59%. Taking into account that savings of 4.3% to 10.2% are obtained through load shifting under different pricing-based demand response programs [52] and up to 30% in energy communities with an internal energy exchange cost integrated into energy community systems [53], FLEMS could be positioned as a potential savings maximizer. However, its most significant benefits are provided by individual participants.

Power Quality Assessment

Despite being outside the scope of this work, a short power quality analysis was carried out on the AC bus to evaluate the harmonic distortion under different operating conditions of the PVZEN microgrid. Voltage and current waveforms were acquired at high resolution and processed through FFT-based harmonic decomposition following the guidelines of IEC 61000-4-7, using portable instrumentation, which specifications are available in [54]. Despite the presence of non-linear loads—primarily the programmable resistive emulator and the electronic equipment connected to the auxiliary lines (electronic switches) —the voltage at the inverter outputs consistently exhibited high power quality.

Across all operating scenarios, the Total Harmonic Distortion of voltage (THD_V) remained in the narrow range of 2.1–2.4%, well below the 8% limit typically prescribed for low-voltage systems. This behavior highlights the

Table 5 Total operational cost for case study 3

Unit	EMS (€)	Without FLEMS (€)	FLEMS (€)
1	0.031	0.036	0.076
2	0.018	0.09	0.108
3	0.029	0.259	0.161
Total	0.078	0.385	0.345

capability of the off-grid inverters to maintain a stable and clean AC waveform both in grid-connected and isolated operation.

As expected, the Total Harmonic Distortion of current (THD_I) measured on the three monitored lines was significantly higher, with typical values of approximately 107%, 75% and 45%, respectively. These values arise from the switching behavior of the load emulator and from the presence of non-linear server power supplies, rather than from any limitation of the inverter or the microgrid infrastructure.Throughout the measurement campaigns, no evidence of harmful harmonic propagation or resonance phenomena was observed, and the power quality remained stable over prolonged periods of operation.

Conclusion

A close-to-real-time (30-second intervals) flexibility management system, based on a unified management approach, was implemented to control and manage the real-time power deviations and the behind-the-meter flexibility of a single prosumer and an energy community, composed of real-world photovoltaic panels, lithium batteries, and inverters operating within the PVZEN microgrid laboratory at Politecnico di Torino. The experimental results presented in this work demonstrate that FLEMS is capable of minimizing the overall energy cost, while reliably and safely providing flexibility services to external agents.

In the case of single prosumer operation, experimental campaigns resulted in cost savings ranging from 81% to 85% during two distinct time intervals characterized by extreme energy imbalance. Concerning the operation of the entire community—comprising three prosumers—the comparison between different energy management strategies revealed a total cost reduction of approximately 12% during the analyzed time frame, which was affected by photovoltaic overproduction and underproduction, as well as variability in inflexible demand.

Additionally, this work introduces new parameters into the CBA to consider the costs and revenues associated with providing flexibility. More generally, the experimental results successfully validate several findings previously reported in [24], which were based on simulations and emulations. Specifically, the sensitivity of the adaptive autoregression algorithm (ARA) to parameters such as sampling time and the number of historical values, as well as the influence of cost models for O&M, aging, and penalty terms, was confirmed under real operating conditions.

A comparative analysis between the performance of FLEMS and the standard inverter operation shows that FLEMS reduces energy injections into the grid, mitigates battery micro-cycling, and lowers aging-related degradation costs. Additionally, FLEMS enables the integration of unexpected electric vehicle (EV) charging sessions without incurring extra costs. According to the implemented algorithms, FLEMS consistently prioritizes the optimal energy schedule generated by the Energy Management System (EMS), which is considered a local optimum within the overall optimization framework. This approach reduces medium- and long-term deviations, as EMS accounts for all relevant variables and constraints over extended time horizons.

Finally, all energy management systems are subject to a minimum latency required to acquire measurements, transmit and process data, and subsequently dispatch updated power setpoints to energy assets. This latency primarily depends on the communication infrastructure and the computational burden of the optimization routine. In the configuration analyzed in this work, the minimum required time for the complete FLEMS operation was found to be under 22 s. As part of future work, the authors could investigate the feasibility of operating the system with shorter sampling intervals to enhance cost savings further.

Author Contributions A.C. and F.S. provided the PVZEN microgrid laboratory with real-world equipment, enabling the corresponding author (J.F.) to conduct the experiments. This work was performed during the doctoral stay of the corresponding author. Additionally, they guided and supervised the development of all the case studies. Besides, A.C. wrote Section 4, and A.C. and F.S. checked the preprint versions. R.V. and F.D. provided important advice about the algorithms, control, and management strategy in a real-time timeframe. F.D. verified the battery model and costs. All authors reviewed the manuscript.

Funding Open Access funding provided thanks to the CRUE-CSIC agreement with Springer Nature. This research is part of Project PLEC2021-008152, funded by MCIN/AEI/10.13039/501100011033 of Ministerio de Ciencia, Innovación y Universidades, and by the European Union "NextGenerationEU"/PRTR".

Data Availability The present work data were deposited into the IEEE Dataport database and are available at the following URL: https://ieee-dataport.org//documents/flems-pvzen

Declarations

Competing interests The authors declare no competing interests.

References

1. Mohandes B, El Moursi MS, Hatziargyriou N, El Khatib S (2019) A review of power system flexibility with high penetration of renewables. IEEE Trans Power Syst 34(4):3140–3155. https://doi.org/10.1109/TPWRS.2019.2897727
2. Bhuiyan R, Weissflog J, Schöpf M, Fridgen G (2022) Indicators for assessing the necessity of power system flexibility: a systematic review and literature meta-analysis. Paper presented at the 18th International Conference on the European Energy Market (EEM):Ljubljana, Slovenia, 2022, pp. 1-7
3. Peng Y, Zhou Q, Qin X, Ding B, Zhang Y (2022) Power System Flexibility Indicators Considering Reliability in Electric Power System with High-Penetration New Energy. Paper presented at the 5th International Conference on Power and Energy Applications (ICPEA):Guangzhou, China, 2022, pp 469-474
4. Domenech CB, De Corato AM, Mancarella P (2024) Co-optimization of behind-the-meter and front-of-meter value streams in community batteries. J Mod Power Syst Clean Energy 12(2), 334–345. https://doi.org/10.35833/MPCE.2023.000746
5. Utkarsh K, Ding F (2022) A peer-to-peer market-based control strategy for a smart residential community with behind-the-meter distributed energy resources. Paper presented at the IEEE Power & Energy Society General Meeting. Denver CO USA PESGM 2022, pp 1–5
6. Akkouch R, Menci SP, Pavic I (2024) Congestion management in European electricity systems through aggregators and local flexibility markets: A systematic literature review. Paper presented at the 20th international conference on the european energy market (EEM), Istanbul, Turkiye, 2024, pp 1-7
7. Renewables EDFP (2021) How front-of-the-meter options provide a flexible path to solar. [Online]. Available in: https://www.powerflex.com/blog/how-front-of-the-meter-options-provide-a-flexible-path-to-solar
8. Lopez-Lorente J, Liu XA, Best RJ, Makrides G, Morrow DJ (2021) Techno-economic assessment of grid-level battery energy storage supporting distributed photovoltaic power. IEEE Access 9:146256–1462805. https://doi.org/10.1109/ACCESS.2021.3119436
9. Srivastava A, Zhao J, Zhu H, Ding F, Lei S, Zografopoulos I, Haider R, Vahedi S, Wang W, Valverde G, Gomez-Exposito A (2025) Distribution system behind-the-meter ders: Estimation, uncertainty quantification, and control. IEEE Trans Power Syst 40(1):1060–1077. https://doi.org/10.1109/TPWRS.2024.3404815
10. Fouladi E, Baghaee HR, Bagheri M, Gharehpetian GB (2025) Power management of microgrids including phevs based on maximum employment of renewable energy resources. IEEE Trans Ind Appl 56(5):5299–5307. https://doi.org/10.1109/TIA.2020.3010713
11. Worku MY, Hassan MA, Abido MA (2019) Real time energy management and control of renewable energy based microgrid in grid connected and island modes. Energies 12(2):276. https://doi.org/10.3390/en12020276
12. Akbari S, Martins J, Camarinha-Matos LM, Petrone G (2019) A two-stage probabilistic flexibility management model for aggregated residential buildings. Energy and Buildings 332:115404. https://doi.org/10.1016/j.enbuild.2025.115404
13. Barja-Martinez S, Rücker F, Aragüés-Peñalba M, Villafafila-Robles R, Munné-Collado Í, Lloret-Gallego P (2021) A novel hybrid home energy management system considering electricity cost and greenhouse gas emissions minimization. IEEE Trans Ind Appl 57(3):2782–2790. https://doi.org/10.1109/TIA.2021.3057014
14. Coudray T (2025) Forecasting power system flexibility requirements a hybrid deep-learning approach. Electric Power Syst Res 241:111307. https://doi.org/10.1016/j.epsr.2024.111307
15. Heider F, Plenz M, Schulz D (2021) Smart Grid Power Management Interface for Use of short-term Flexibility. Paper presented at the 9th International Conference on Smart Grid (icSmartGrid):Setubal, Portugal, 2021, pp 82-91
16. Asghari AHB, Sharma RK (2014) Experimental demonstration of a tiered power management system for economic operation of grid-tied microgrids. IEEE Trans Sustain Energy 5(4):1319–1327. https://doi.org/10.1109/TSTE.2014.2339132
17. Ma J, Silva V, Belhomme R, Kirschen DS, Ochoa LF (2012) Exploring the use of flexibility indices in low carbon power systems. Paper presented at the 3rd IEEE PES Innovative Smart Grid Technologies Europe. Berlin Germany ISGT Europe 2012, pp 1–5
18. Gazafroudi AS, Prieto-Castrillo F, Pinto T, Corchado JM (2018) Energy flexibility management in power distribution systems: decentralized approach. Paper presented at the International Conference on Smart Energy Systems and Technologies (SEST). Seville, Spain, 2018, pp 1-6
19. Suljanovic AMN, Zajc M (2025) Quantifying the impact of flexibility asset location on services in the distribution grid: Power system and local flexibility market co-simulation. Electr Power Syst Res 238:111037. https://doi.org/10.1016/j.epsr.2024.111037
20. Nolzen N, Ganter A, Baumgärtner N, Baader FJ, Leenders L, Bardow A (2025) Where to market flexibility? integrating continuous intraday trading into multi-market participation of industrial multi-energy systems. Comput Chem Eng 195:109026. https://doi.org/10.1016/j.compchemeng.2025.109026
21. Bremdal BA, Sæle H, Mathisen G, Degefa MZ (2018) Flexibility offered to the distribution grid from households with a photovoltaic panel on their roof: Results and experiences from several pilots in a Norwegian research project. IEEE International Energy Conference (ENERGYCON). Limassol Cyprus 2018, pp 1–6
22. IEEE (2018) IEEE standard for the specification of microgrid controllers. IEEE Std 2030.7-2017, pp 1-43, 23-April-2018
23. IEEE (2018) IEEE Standard for the Testing of Microgrid Controllers. IEEE Std 2030.8-2018, pp 1-42, 24-Aug-2018
24. Forero-Quintero JF, Villafafila-Robles R, Barja-Martinez S, Codina-Escolar M, Montesinos-Miracle D (2023) A flexibility management system for behind-the-meter flexibility with distributed energy resources: A sensitivity analysis. Sustain Energy Technol Assess 60:103404. https://doi.org/10.1016/J.SETA.2023.103404
25. Barragán DE, Acurio BA, López JC, Grijalva F, Rodríguez JC, da Silva LC (2022) An energy management system for a residential microgrid using convex optimization. Paper presented at the IEEE Sixth Ecuador Technical Chapters Meeting (ETCM):Quito. Ecuador 2022, pp 1–5
26. Akarne Y, Essadki A, Nasser T, El Bhiri B (2024) Experimental analysis of efficient dual-layer energy management and power control in an ac microgrid system. IEEE Access 12:30577–30592. https://doi.org/10.1109/ACCESS.2024.3370681
27. Beus M, Herenčić L, Pandžić H, Rajšl I (2022) Laboratory setup for stability and optimization studies of hybrid microgrids. Paper presented at the 7th International Conference on Smart and Sustainable Technologies (SpliTech):Split / Bol, Croatia, 2022, pp 1-6
28. Buraimoh E, Ozkan G, Timilsina L, Muriithi G, Arsalan A, Papari B, Moghassemi A, Edrington C, Ozden M (2024) Distributed deep deterministic policy gradient agents for real-time energy management of DC microgrid. Paper presented at the IEEE Sixth International Conference on DC Microgrids (ICDCM):Columbia, SC, USA, 2024, pp 1-5
29. Prieto-Araujo E, Olivella-Rosell P, Cheah-Mañe M, Villafafila-Robles R, Gomis-Bellmunt O (2015) Renewable energy emulation concepts for microgrids. Renew Sustain Energy Rev 50:325–345. https://doi.org/10.1016/j.rser.2015.04.101

30. Martin-Martínez F, Sánchez-Miralles A, Rivier M (2016) A literature review of microgrids: A functional layer based classification. Renew Sustain Energy Rev 62:1133–1153. https://doi.org/10.1016/j.rser.2016.05.025
31. Olivella-Rosell P, Lloret-Gallego P, Munné-Collado Í, Villafafila-Robles R, Sumper A, Ottessen SØ, Rajasekharan J, Bremdal BA (2018) Local flexibility market design for aggregators providing multiple flexibility services at distribution network level. Energies 11(4):822. https://doi.org/10.3390/en11040822
32. Murugesan S, Jenisha CT, Ponraj P (2024) In-direct communication through disturbance injection based islanding detection strategy. In: IEEE 4th International conference on sustainable energy and future electric transportation, SEFET 2024, Hyderabad, India, 2024, pp 01-06
33. Maganti S, Padhy NP (2024) An advanced control strategy for enhancing voltage support with minimum active power curtailment during asymmetrical faults. IEEE Trans Power Syst 3496472. https://doi.org/10.1109/TPWRS.2024.3496472
34. Pattanaik V, Malika BK, Rout PK, Sahu BK (2023) Contingency-resilient pmu placement using fuzzy logic and discrete artificial bee colony algorithm for comprehensive network observability. e-Prime - Adv Electr Eng Electron Energy 5:100275. https://doi.org/10.1016/j.prime.2023.100275
35. Academy S (2025) Zero injection solutions for on-grid inverters. [Online]. Available: https://kb.solaxpower.com/solution/detail/ff808081899c15cb0189a9b1dc6f00c1 Accessed 16-October-2025
36. Koduru SS, Machina VS, Madichetty S (2022) A Review on Forecasting Models and Anomaly Detection for Household Energy Consumption. In: 2022 International conference on smart generation computing, communication and networking (SMART GENCON):Bangalore, India, 2022, pp 1–6
37. Qiao Q, Yunusa-Kaltungo A, Edwards R (2020) Hybrid method for building energy consumption prediction based on limited data. In: 2020 IEEE PES/IAS PowerAfrica. Nairobi Kenya 2020, pp 1–5
38. Chen H, Xiong R, Lin C, Shen W (2021) Model predictive control based real-time energy management for hybrid energy storage system. CSEE J Power Energy Syst 7(4):862–874. https://doi.org/10.17775/CSEEJPES.2020.02180
39. Elkazaz M, Sumner M, Thomas D (2019) Real-time energy management for a small scale pv-battery microgrid: Modeling, design, and experimental verification. Energies 12(14):2712. https://doi.org/10.3390/en12142712
40. Samuel O, Javaid N, Khalid A, Khan WZ, Aalsalem MY, Afzal MK, Kim BS (2020) Towards real-time energy management of multi-microgrid using a deep convolution neural network and cooperative game approach. IEEE Access 8:161377–161395. https://doi.org/10.1109/ACCESS.2020.3021613
41. MathWorks (2025) FMINCON. Find minimum of constrained nonlinear multivariable function. [ONLINE]. https://www.mathworks.com/help/optim/ug/fmincon.html
42. PVZEN (2025) PVZEN, PhotoVoltaic Zero Energy Network Laboratory, Politecnico di Torino. [Online]. Available: https://pvzen.polito.it/ Accessed: 5-April-2025
43. Di Leo P, Malgaroli G, Amato A, Schubert S, Ciocia A, Spertino F. (2023) An academic laboratory for all-electric energy communities: the case study of PVZEN microgrid. Paper presented at the IEEE 64th international scientific conference on power and electrical engineering of Riga Technical University (RTUCON). Riga, Latvia, 2023, pp 1–6
44. Amato A, Carullo A, Ciocia A, Corbellini S, Spertino F, Vallan A, Bertonasco MA (2025) The pvzen lab for energy communities: Monitoring system for identification of photovoltaic/battery/converter energy models. IEEE Trans Instrum Meas 74:1–12. https://doi.org/10.1109/TIM.2025.3545847
45. Wang J, Liu B, Gong D, He W (2025) Research on the real-time monitoring system for traction force during cable laying process. Paper presented at the 4th international conference on power system and energy technology (ICPSET). Chengdu, China, 2025, pp 322-327
46. Centre ECJR (2025) Photovoltaic geographical information system (PVGIS). [Online]. Available: https://ec.europa.eu/jrc/en/pvgis
47. Labs G (2025) Grafana: The open observability platform. [Online]. Available: https://grafana.com
48. Base DD (2025) Dataport data base. [Online]. Available: https://dataport.cloud Accessed: 7-Sept-2022
49. Agrela JC, Soares T, Villar J, Rezende I. (2025) Local flexibility markets for energy communities: flexibility modelling and pricing approaches. Paper presented at the 21st international conference on the European energy market (EEM):Lisbon, Portugal, 2025, pp 1-7
50. Celik B, Rostirolla G, Caux S, Renaud-Goud P, Stolf P (2019) Analysis of demand response for datacenter energy management using ga and time-of-use prices. In: Proc. 2019 IEEE PES Innov. Smart Grid Technol Eur ISGT-Europe 2019, pp 1–5. https://doi.org/10.1109/ISGTEurope.2019.8905618
51. Nizami MSH, Hossain MJ, Amin BMR, Kashif M, Fernandez E, Mahmud K (2019) Transactive energy trading of residential prosumers using battery energy storage systems. In: 2019 IEEE Milan PowerTech. PowerTech 2019, pp 14–19. https://doi.org/10.1109/PTC.2019.8810458
52. Park H, Bae S, Chang M, Park SH, Yoon GG (2019) A Community-scale Energy Management System for Demand Response Participation of Households with DERs and EVs. In: 2019 IEEE 4th international future energy electronics conference (IFEEC):Singapore, 2019, pp 1-5
53. Alavijeh NM, Alemany DSC, Le Benayas, AT (2019) Impact of internal energy exchange cost on integrated community energy systems. In: 2019 IEEE sustainable power and energy conference (iSPEC). Beijing China 2019, pp 2138–2143
54. Spertino F, Ciocia A, Di Leo P, Tommasini R, Berardone I, Corrado M, Infuso A, Paggi M (2015) A power and energy procedure in operating photovoltaic systems to quantify the losses according to the causes. Sol Energy 118:313–326. https://doi.org/10.1016/j.solener.2015.05.033